Proc. IUTAM symposium on Mesoscopic Dynamics in Fracture Process and Strength of Materials, Osaka, July 2003

A NEW MODEL OF SCALE DEPENDENT CRYSTAL PLASTICITY ANALYSIS

Tetsuya Ohashi

Kitami Institute of Technology,
Koencho 165, Kitami, 090-8507, Japan
E-mail: ohashi@newton.mech.kitami-it.ac.jp

Abstract: Crystal plasticity analysis of slip deformation in metal microstructure enables one to calculate densities for the statistically stored (SS) and the geometrically necessary (GN) dislocations, and such densities are utilized to evaluate the critical resolved shear stresses for slip systems. In this paper, we propose a new model, where the mean free path of moving dislocations is defined as a function of the densities for SS and also, GN dislocations, and the critical resolved shear stresses for slip systems are given only by SSDs. Scale dependent characteristics of GN dislocations is transmitted to the SSDs via the mean free path and finally, to the slip resistance of slip systems. Tensile deformations of six-grained multicrystal models whose average grain diameter, $\overline{d}$, ranges from 0.1 to 500 μm, are analyzed with this new model and micro- and macroscopic aspects are examined. Plastic flow stresses increase almost linearly with $\overline{d}^{-1/2}$ within the range, $500 > \overline{d} > 1\ \mu m$, showing the Hall-Petch relation, and this grain refinement effect is gradually reduced for finer microstructures.

Key words: metal microstructure, crystal plasticity analysis, dislocations, scale dependent plasticity.

1. INTRODUCTION

Scale dependent characteristics of yield stress, plastic flow stress, or indentation hardeness of metal polycrystals are well known and they are summarized in the Hall-Petch type description:

$$\sigma = \sigma_0 + k / \sqrt{\overline{d}} \ ,$$

where, σ_0 and k are considered to be material constants, while $\overline{d}$ is a representative length of material's microstructure. A lot of efforts have been made to establish theoretical framework of solid mechanics that show material scale dependency and among them, a model by Fleck *et al.* (1994) induced a wider range of discussion. In their model, the critical resolved shear stresses of slip systems are modeled by the ordinary Taylor type expression but they introduced the geometrically necessary (GN) dislocations as well as the statistically stored (SS) ones into it. That is,

$$(\textit{critical resolved shear stress}) \propto \sqrt{\rho_S + \rho_G}$$

where, ρ_S and ρ_G denote the densities of the SS and GN dislocations, respectively. Density increment of the SS dislocations is related to the increment of plastic shear strain and the mean free path of moving dislocations, while the density of the GN ones is related to the spatial gradient of the plastic shear strain on slip systems. The critical resolved shear stress reflects its scale dependent characteristics of the GN dislocations through the above expression. However, it is still open to discussion whether the above expression is valid and sufficient (for example, Weertman, 2002, and Needleman and Gil Sevillano, 2003).

In this paper, we propose a new model of scale dependent crystal plasticity analysis, where the mean free path of moving dislocations is defined as a function of the densities for SS and also, GN dislocations, and the critical resolved shear stresses for slip systems are given only by SS dislocations. Scale dependent characteristics of GN dislocations is transmitted to the SS dislocations via the mean free path and finally, to the slip resistance of slip systems. Tensile deformations of six-grained multicrystal models whose average grain diameter, $\overline{d}$, ranges from 0.1 to 500 μm, are analyzed with this new model and micro- and macroscopic aspects are examined.

2. BASIC EQUATIONS

Slip deformation is assumed to take place on {111} crystal plane and in <110> crystal direction. The activation condition of the slip system *n* is given by the Schmid law;

$$P_{ij}^{(n)}\sigma_{ij} = \theta^{(n)}, \quad P_{ij}^{(n)}\dot{\sigma}_{ij} = \dot{\theta}^{(n)}, \quad (n = 1,\cdots,12), \qquad (1)$$

and,

$$P_{ij}^{(n)} = \frac{1}{2}\left(\nu_i^{(n)} b_j^{(n)} + \nu_j^{(n)} b_i^{(n)}\right), \tag{2}$$

where, σ_{ij} and $\theta^{(n)}$ denote the stress and the critical resolved shear stress on the slip system n, respectively. The slip plane normal $\nu_i^{(n)}$ and the slip direction $b_i^{(n)}$ define the Schmid tensor $P_{ij}^{(n)}$. Quantities with dot indicate increments of them. Increment of the critical resolved shear stress is written as follows;

$$\dot{\theta}^{(n)} = \sum_m h^{(nm)} \dot{\gamma}^{(m)}. \tag{3}$$

Here, $\dot{\gamma}^{(m)}$ denotes the increment of plastic shear strain on slip system m. If the deformation is small and rotation of the crystal orientation is neglected, the constitutive equation is written as follows (Hill, 1966),

$$\dot{\sigma}_{ij} = [S_{ijkl}^e + \sum_n \sum_m \{h^{(nm)}\}^{-1} P_{ij}^{(n)} P_{kl}^{(m)}]^{-1} \dot{\varepsilon}_{kl}. \tag{4}$$

S_{ijkl}^e denotes elastic compliance. Summation is made over the active slip systems.

Let us suppose that the critical resolved shear stress is given by the following equation (Ohashi, 1987, 1994);

$$\theta^{(n)} = \theta_0 + \sum_m \Omega^{(nm)} a \mu \tilde{b} \sqrt{\rho_S^{(m)}}, \tag{5}$$

where, θ_0 denotes the lattice friction term, which is, in general, very small for fcc crystals, and $\rho_S^{(m)}$ denotes the density of SS dislocations that accumulate on the slip system m. Reaction between dislocations on slip systems n and m defines the magnitude of the interaction matrix $\Omega^{(nm)}$. Diagonal terms in $\Omega^{(nm)}$ are unity and in the present study, we choose off diagonal terms to express pseudo-isotropic hardening character for every slip system[1]. μ and $\tilde{b}$ denote the elastic shear modulus and magnitude of Burgers' vector, respectively. a is a numerical factor, which is close to 0.1.

---

[1] To ensure the existence of the inverse of the hardening coefficient, which will be given in eq. (11), we also introduce a numerical "noise" of the order of 10^{-4} in $\Omega^{(nm)}$.

Increment of the SS dislocations is given as follows;

$$\dot{\rho}_S^{(n)} = c\dot{\gamma}^{(n)} \Big/ \tilde{b}L^{(n)}, \tag{6}$$

where, c is a numerical coefficient of the order of 1. $L^{(n)}$ denotes the mean free path of dislocations on slip system n and, in this paper, we use the following model for it;

$$L^{(n)} = \frac{c^*}{\sqrt{\sum_{m \neq n} \left(s \cdot \rho_S^{(m)} + g \cdot \left\| \rho_G^{(m)} \right\| \right)}}, \tag{7}$$

where, c^* is a material constant of the order of 10 - 100 (for detailed discussion, Kuhlmann-Wilsdorf, 1989) . Parameters s and g are introduced to control the analysis and $0 \leq s \leq 1$, $0 \leq g \leq 1$.[2]

The edge and screw components of the geometrically necessary dislocations are obtained from the strain gradients (Ohashi, 1997);

$$\rho_{G,edge}^{(n)} = -\frac{1}{\tilde{b}} \frac{\partial \gamma^{(n)}}{\partial \xi^{(n)}}, \qquad \rho_{G,screw}^{(n)} = \frac{1}{\tilde{b}} \frac{\partial \gamma^{(n)}}{\partial \zeta^{(n)}}. \tag{8}$$

Here, $\xi^{(n)}$ and $\zeta^{(n)}$ denote directions parallel and perpendicular to the slip direction on the slip plane, respectively. Norm of two components defines the scalar density for the GN dislocations,

$$\left\| \rho_G^{(n)} \right\| = \sqrt{\left(\rho_{G,edge}^{(n)} \right)^2 + \left(\rho_{G,screw}^{(n)} \right)^2}. \tag{9}$$

Evaluation of the edge and screw components for the GN dislocations enables one to calculate the tangent vector $\mathbf{l}^{(n)}$ of the dislocation line segments (Ohashi, 1999);

$$\mathbf{l}^{(n)} = \frac{1}{\left\| \rho_G^{(n)} \right\|} \left(\rho_{G,screw}^{(n)} \cdot \mathbf{b}^{(n)} + \rho_{G,edge}^{(n)} \cdot \mathbf{b}^{(n)} \times \mathbf{v}^{(n)} \right). \tag{10}$$

---

[2] A similar approach was made by Acharya and Beaudoin (2000). In their model, total dislocation density was given by geometrically and statistically determined densities; mean free paths for the former quantity was determined by the slip plane lattice incompatibility and the latter by density of the total forest dislocations.

Data for GN dislocations are obtained for each finite element and then, we can draw line segments of dislocations in three-dimensional space. We will draw one line segment at the center of each element. Direction of the line segment is given by eq. (10) and its length and thickness are determined by the density norm $\left\|\rho_G^{(n)}\right\|$.

The strain hardening coefficient in equation (3) is given by the following equation;

$$h^{(nm)} = \frac{1}{2} ac\mu\,\Omega^{(nm)} / \left[L^{(m)} \sqrt{\rho_S^{(m)}} \right], \tag{11}$$

and by substituting eq. (7) into eq. (11), we have

$$h^{(nm)} = \frac{ac\mu}{2c^*}\,\Omega^{(nm)} \sqrt{\frac{\sum_{k \neq m} \left(s \cdot \rho_S^{(k)} + g \cdot \left\|\rho_G^{(k)}\right\|\right)}{\rho_S^{(m)}}}\,. \tag{12}$$

Table 1. Euler angles for crystal grain 1-6, and their Schmid factor for the primary and critical slip systems.

grain	Euler angle			Schmid factor	
	κ	θ	ϕ	primary	critical
1	85.5	24.0	212.9	0.4968	0.4862
2	80.0	16.0	101.4	0.4881	0.4775
3	53.3	13.6	215.3	0.4632	0.4416
4	88.5	35.6	182.9	0.4665	0.4593
5	56.3	17.7	219.4	0.4747	0.4397
6	68.1	5.71	213.1	0.4426	0.4398

3. RESULTS AND DISCUSSION

3.1 Microscopic aspects of slip deformation in six-grained multicrystals

Figure 1(a) shows the six-grained multicrystal model employed in this study. Ratio of the width (w), height (h), and thickness (d) of the specimen is w:h:d=5:15:1. We made nine specimens of similar shape but with different dimensions: the width w of the specimens are 0.1, 0.2, 0.5, 1, 2.5, 5, 50, 100, and 500 μm. The average grain diameters $\overline{d}$ of the models are approximately equal to w. The models are divided into finite elements and their tensile deformations in y direction are analyzed by our crystal plasticity

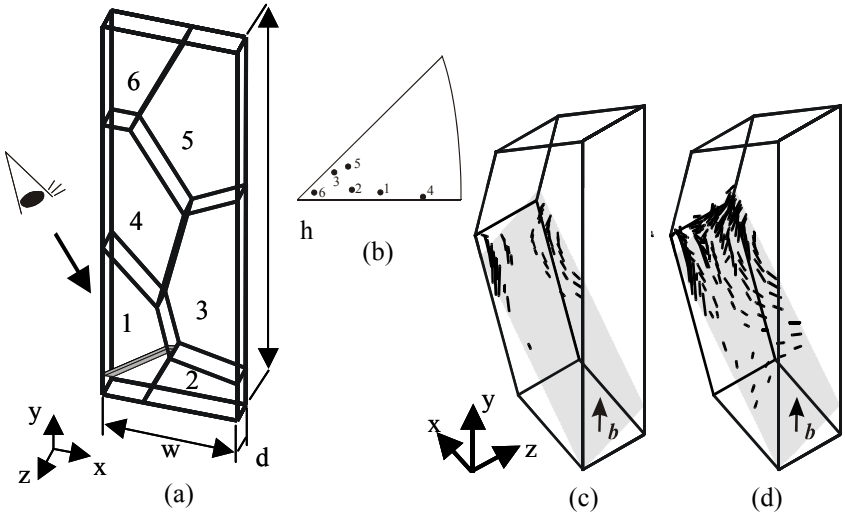

Fig.1 (a):Six-grained multicrystal model employed in this study and a thin foil region in the grain 1. The foil is cut parallel to the primary slip plane. (b): crystal orientations. (c),(d):Development of GN dislocations on the primary system when the average tensile strain is 0.049 and 0.053 %, respectively.

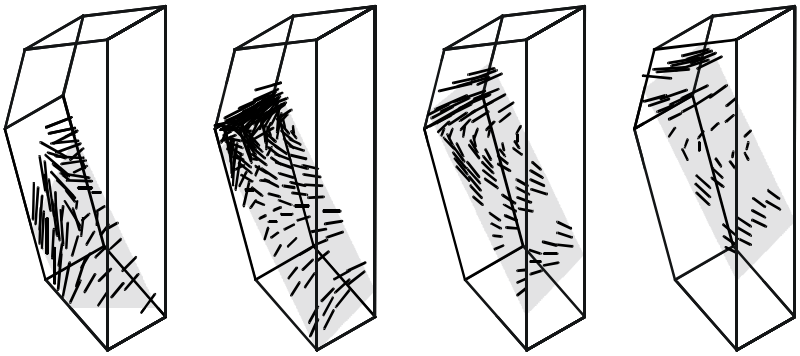

Fig.2 (a) - (d): Three-dimensional distribution of the GN dislocations on the primary system when the average tensile strain is 0.068 %.

software code *clp7*. We use a fine mesh (4864 elements in total) for detailed study of microscopic aspects of slip at small strain range, and a coarse one (480 elements) to calculate macroscopic response of the whole specimen up to 20% strain. Elastic compliance data for Cu are used for the six grains and the initial dislocation densities for twelve slip systems are supposed to be $1x10^{12}$ m^{-2} and c*=100 in all the specimens. Crystal orientations are shown in Figure 1(b) and Schmid factors for the primary and a secondary slip system are summarized in Table1.

First, we examine slip deformation in detail by scale independent (*s*=1,

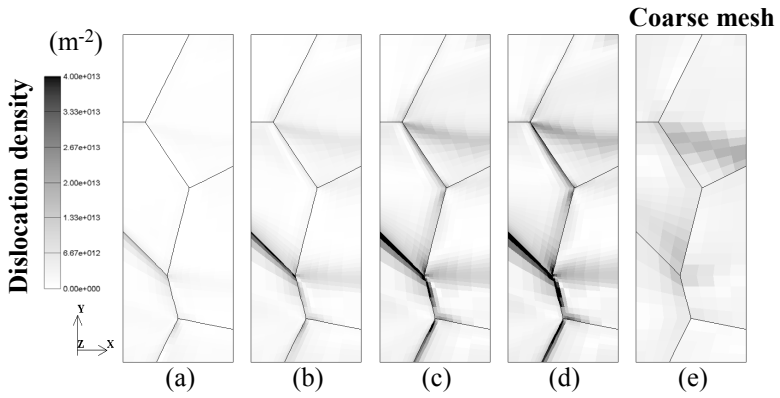

Fig.3 (a) - (d): Density distribution of the GN dislocations on the primary system when the average tensile strain is 0.08, 0.16, 0.32, and 0.4 %, respectively. The fine mesh is used. (e):Result obtained by the coarse mesh. The average tensile strain is 0.4%.

g=0) hypothesis. Figures 1(c) and (d) show development of GN dislocations in a thin foil in the grain-1 at the very beginning of plastic slip deformation. The foil is parallel to the primary system and positioned as illustrated in Figure 1(a). Viewing direction of Figs.1(c) and (d) is also given in Fig.1(a). When the average tensile strain is about 0.049%, slip deformation starts near a grain boundary triple junction. Segments of GN dislocations make up half loop shaped structures. As the deformation proceed (Figure 1(d)), the loop shaped structure grows and dislocation pile-up is observed near the triple junction. The shape of GN dislocation segments in places far apart from the triple junction is rather straight. Figures 2(a)-(d) compare the structure of GN dislocations in different positions. Dislocation pile-ups at grain boundaries are commonly observed, but other features differ gradually from place to place. Figures 3(a)-(d) show growth of accumulation of GN dislocations when the average tensile strain is less than 0.4%. Not only grain boundary pile-ups, but also a formation of thin region of higher density growing straight from some grain boundary triple junctions are observed. The latter type of structure is supposed to be formed by many body interaction of crystal grains; interaction of at least three crystal grains contribute to the formation of this type of structure (Ohashi, 1989). Fig 3(e) shows the result obtained with the coarse finite element mesh, as a comparison to Fig. 3(d). Details of grain boundary pile-ups are not clear in the result by the coarse mesh, while densities at grain interior shows to be approximately equal to the ones obtained by the fine mesh.

3.2 Scale dependent analysis

We now analyze slip deformation with the scale dependent model by setting s=g=1 in eq. (7). We use a coarse mesh, which enables us to

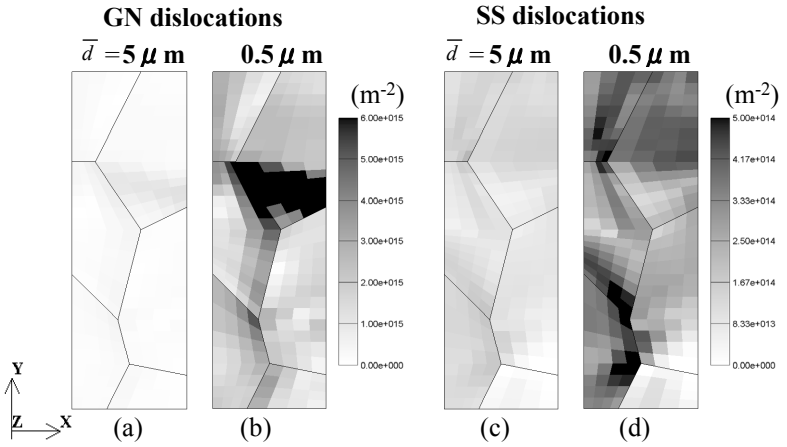

Fig.4 (a),(b): Density distribution of the GN dislocations on the primary system when the average tensile strain is about 19%. The average grain diameter is 5 and 0.5 μm, respectively. (c),(d): Density distribution of the SS dislocations on the primary system when the average tensile strain is about 19%. The average grain diameter is 5 and 0.5 μm, respectively.

analyze the deformation up to 20% tensile strain in a realistic computer time. With this coarse mesh, some details of dislocation structure will be missing, on which we made a comparison in Figures 3(d) and (e). Effects of such a fine structure of dislocations on the macroscopic response of the specimen are not fully understood and a point of interest for further study.

Figures 4(a)-(d) compare results for the GN and SS dislocations obtained for specimens with average grain sizes of 5 and 0.5 μm. Specimens are deformed until the average tensile strain is about 19%. It should be noted that color bars used in these figures are different from each other and also from the one used in Figures 3. Densities of GN dislocations in the specimen of $\bar{d}$ =0.5 μm is about 10 times as large as the ones in the $\bar{d}$ =5 μm specimen, which is a logical consequence of the theory that we evaluate the GN dislocations. At the same time, densities of SS dislocations in the specimen of $\bar{d}$ =0.5 μm is about 5 times as large as the ones in the $\bar{d}$ =5 μm specimen and this cause higher flow stress for specimen with smaller grain size.

Figure 5 shows nominal stress - strain curves for specimens with different mean grain diameters. Yield stresses for the all specimens are substantially the same, but the strain hardening is more significant for specimens with smaller grain size. Differences in strain hardening characteristics for specimens with $\bar{d}$ >50 μm and scale independent models are negligibly small, while the strain hardening of the specimens with sub-micron grain diameter becomes remarkably high with the reduction of the mean grain diameter. Figure 6 shows the flow stress at 20% tensile

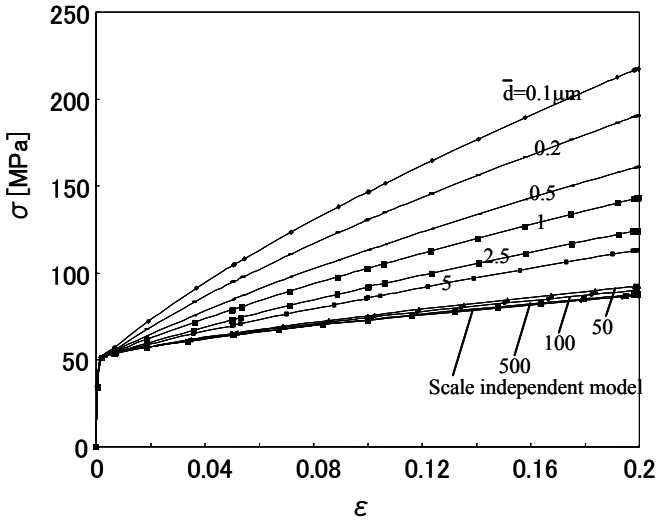

Fig.5 Nominal stress - strain response of specimens with various mean grain diameter.

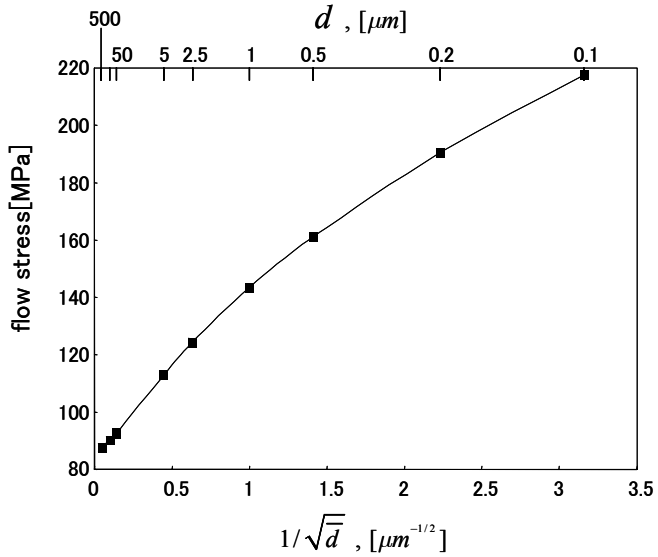

Fig.6 Hall-Petch plot of the flow stresses when the mean tensile strain is about 20%.

strain plotted against $1/\sqrt{\bar{d}}$. The flow stress increase almost linearly within the range $\bar{d}$ >1 μm , showing a Hall-Petch relation, and the slope gradually decreases when $\bar{d}$ is smaller than 1 μm. If we apply the Hall-Petch relation for the flow stress data for the specimens of $\bar{d}$ >1 μm, the coefficient k is calculated as about 1.84 MPa-mm$^{1/2}$ (=5.82x10^{-2} MPa-m$^{1/2}$). This is about a half of the data obtained by experiment for Al (Ono, *et al.*, 2002). Number of crystal grains in the thickness direction is unity in the present multicrystal model, and mutual constraint of their

deformation is quasi two-dimensional. On the other hand, three-dimensional constraint of deformation will generally be taking place in polycrystals. This difference in mutual constraint between crystal grains will make a significant change in the strain hardening phenomenon and its scale dependency. This point should be explored in future work. Also, the parameter c* and the initial densities of SS dislocations will have effects on the strain hardening, as eq. (12) implies. Then, the effects of c* and the initial densities of SS dislocations and its non-uniform distribution on the strain hardening phenomenon are also issues of future studies. It is a well known phenomenon that the Hall-Petch relation fails for sub-micron and nanometer regions. A full understanding of its mechanism has not been obtained, although it is usually attributed to grain boundary sliding. It was shown in the present analysis that some mechanism other than grain boundary sliding can contribute to the decrease of the k value for the region $\overline{d}$ <1 μm. Then, it seems to be interesting to examine how the strain hardening and the scale dependency occur in microstructures with sub-micron sizes. Scale dependent characteristics of the yield stress is another important point for further study.

4. SUMMARY

We made a new scale dependent crystal plasticity model, where not only the statistically stored but also the geometrically necessary dislocations contribute to the mean free path of moving dislocations. Obtained results showed an approximately linear relationship between the inverse of the square root of the mean grain diameter of multicrystal models and the flow stress for the range that the mean grain diameter was larger than 1 μm. For smaller grain sizes, the grain refinement effect was gradually reduced.

References

Acharya, A. and Beaudoin, A.J., 2000, J. Mech. Phys. Solids, **48**, 2213.
Fleck, N.A., *et al.*, 1994, Acta metall. mater., **42**, 475.
Hill, R. 1966, J. Mech. Phys. Sol., **14**, 95-102.
Kuhlmann-Wilsdorf, D., 1989, Mat. Sci. Eng. **A113**, 1.
Needleman, A. and Gil Sevillano, J., 2003, Scripta Mat., **48**, 109.
Ohashi, T., 1987, Trans. Japan Inst. Met. **28**, 906.
Ohashi, T., 1990, Colloque de Physique, Col. C1, **51**, c1-593.
Ohashi, T., 1994, Phil. Mag., **A70**, 793.
Ohashi, T., 1997, Phil. Mag. Lett., **75**, 51.
Ohashi, T., 1999, J. Phys. IV France, **9**, Pr9-279.
Weertman, J., 2002, Acta Mat., **50**, 673.